

# The Couette flow of dense and fluid-saturated granular media

Pierre-Yves Lagrée \*, Daniel Lhuillier

*Laboratoire de Modélisation en Mécanique UPMC-CNRS, Boîte 162, 4, place Jussieu, 75252 Paris cedex 05, France*

Received 19 October 2005; received in revised form 17 March 2006; accepted 21 March 2006

Available online 11 May 2006

---

## Abstract

A continuum-mechanical description is proposed for *dense* granular media submitted to *steady* shears. By dense granular media we mean high solid fractions in the range between the random loose and the random close packings. The description is based on a modeling of the stresses resulting from free-volume entropic effects, contacts and impacts between particles, and viscosity of the interstitial fluid. The non-homogeneity of the material is taken into account via several transport coefficients depending on the solid fraction. When applied to the tangential annular flow in a Couette cell, the model predicts velocity and solid fraction profiles which agree qualitatively with those found experimentally but which also present some conflicting features, possibly due to the difficulties to achieve a true steady profile for the solid fraction. More precisely, we obtain the following predictions: (a) a minimum shear is required for motion, (b) above this minimum the motion is localized and the solid fraction decreases when approaching the inner moving cylinder, (c) the width of the shear band increases with the applied shear stress up to a maximum value above which our description fails because the solid fraction at the inner moving cylinder becomes smaller than the random loose packing, (d) the maximum width of the shear band is proportional to the radius of the inner cylinder, with a proportionality coefficient which increases with the fluid viscosity and decreases with the confining pressure and the grain size, (e) for dry granular media the maximum width of the shear band is approximately half the radius of the inner cylinder so that localization is observed in almost all Couette cells, (f) when a very viscous fluid surrounds the grains the width of the shear band often exceeds the gap of the Couette cell, giving the (wrong) impression that shear localization has disappeared.

© 2006 Elsevier Masson SAS. All rights reserved.

*Keywords:* Wet granular systems; Rheology; Couette flow

---

## 1. Introduction

A Couette cell is certainly amongst the most convenient devices for determining the steady flow behavior of complex materials. The main specificity of dense granular media is their localized motion, the so-called shear localization. And the main difficulty with granular media is their opacity which explains why the first experiments were mostly two-dimensional [1] or limited to the observation of the upper or bottom surfaces [2]. Then, magnetic resonance imaging and X-ray tomography allowed true three-dimensional measurements [3,4]. The main conclusions of these 2D or 3D experiments were the exponential-like (or Gaussian-like) velocity profile in the shear band, and the decrease of the compaction close to the moving inner cylinder. Shear flow in a Couette cell has recently been studied with liquid-

---

\* Corresponding author.

*E-mail address:* [pyl@ccr.jussieu.fr](mailto:pyl@ccr.jussieu.fr) (P.-Y. Lagrée).

saturated granular media [5,6]. The interstitial fluid was found to increase the width of the shear band and, seemingly to suppress any localization of the motion. These surprising results, together with the finding of a universal velocity profile for wet and dry materials, prompted us to extend a model initially proposed for dry materials [7] to include the role of an interstitial fluid. The model we have developed is based on a suggestion made long ago by Savage [8] and Johnson and Jackson [9], who split the stress tensor into a rate-independent part related to free-volume phenomena and a rate-dependent part due to the contact forces between particles (see also the related model of Ancey and Evesque [10]). The resulting stress involves several transport coefficients depending on the grain volume fraction. We have renewed that approach by refining the expressions of these transport coefficients. We already tested the model in flows over heaps or rough inclines [7]. Here we want to detail the predictions for the Couette flow.

The general features of the motion in a Couette cell are briefly reviewed in Section 2, while the model for dense granular media is presented in Section 3. The generic velocity and solid fraction profiles are obtained in Section 4. The predictions of the model are presented in Section 5 for two important limit-cases (constant confining pressure and constant mean volume fraction), and they are compared with the experimental results of [5,6].

## 2. Pressure and shear stresses in a Couette cell

A widely used apparatus to study the rheology of continuous media is the Couette cell, made of two co-axial vertical cylinders with radii  $r_{\text{int}}$  and  $r_{\text{ext}}$ . The inner cylinder rotates and imparts momentum to the medium bounded by the two cylinders. Once in a steady state, the medium moves with an angular velocity  $\omega(r, z)$ , a shear rate  $r \partial \omega / \partial r$  and an azimuthal velocity  $r \omega(r, z)$ . Mass conservation is automatically satisfied. Momentum conservation simplifies considerably when assuming that the stress tensor  $\tau$  is symmetric and has vanishing components  $\tau_{zr}$  and  $\tau_{z\theta}$ . These assumptions are far from trivial in case of granular media: a rough boundary prevents the grains to rotate freely (meaning that their mean angular velocity is possibly different from  $\omega$ ) and the stress tensor is presumably not symmetric at distances less than a few diameters from it. Moreover the assumption of a vanishing  $\tau_{zr}$  means the neglect of any Janssen-like effect in the Couette cell (i.e. no vertical friction forces on the cylinders). When these assumptions are taken for granted, momentum conservation reduces to

$$\begin{aligned} r \partial \tau_{rr} / \partial r + \tau_{rr} - \tau_{\theta\theta} &= \rho r^2 \omega^2, \\ \partial (r^2 \tau_{r\theta}) / \partial r &= 0, \\ \partial \tau_{zz} / \partial z &= \rho g, \end{aligned}$$

in the radial, azimuthal and axial direction respectively. For fluid-saturated granular media the mass per unit volume is  $\rho = \phi \rho_p + (1 - \phi) \rho_f$  where  $\phi$  is the volume fraction of the grains while  $\rho_p$  and  $\rho_f$  are the mass per unit volume of the grains and the interstitial fluid respectively. The momentum conservation in the radial direction implies

$$\tau_{rr}(r_{\text{ext}}, z) = \tau_{rr}(r_{\text{int}}, z) + \int_{r_{\text{int}}}^{r_{\text{ext}}} (\tau_{\theta\theta} - \tau_{rr} + \rho r^2 \omega^2) \frac{dr}{r}. \tag{1}$$

Because of the very slow motion we will assume that the normal stress difference  $\tau_{rr} - \tau_{\theta\theta}$  and the centrifugal pressure have a negligible role. These assumptions are supported by the direct observation of the free-surface which appears to stay horizontal without any deformation, at the least for  $\omega < 1$  rad/sec. As a consequence, the momentum conservation of slowly moving and dense granular media simply expresses as

$$\tau_{rr} \approx N(z), \tag{2}$$

$$\tau_{r\theta} \approx S(z) \left( \frac{r_{\text{int}}}{r} \right)^2, \tag{3}$$

where  $N(z)$  and  $S(z)$  are the pressure and shear stress on the inner cylinder.

### 3. Constitutive relations

#### 3.1. Dry granular media

A dense granular medium is one in which contacts between grains are long-lived and lead to a contact network spanning all over the sample. This requires a minimum volume fraction  $\phi_m$  which is likely to be the random loose packing (of order 0.55 for spherical grains). When its volume fraction is larger than  $\phi_m$ , the medium displays a compressibility which is not linked to the elasticity of the grains, but stems from the free volume available and the exploration of many microstates with different configurations of the grains. This irrelevance of the elastic properties of the grains is an approximation which holds up to a volume fraction  $\phi_M$  which is equal or slightly smaller than the random close packing (of order 0.65 for spherical grains). The constitutive relations to be presented below are those prevailing in the *dense* solid fraction range  $\phi_m \leq \phi \leq \phi_M$ . A second and important restriction is their limitation to *steady* shear flows. As a consequence, velocity fluctuations and the fluctuational kinetic energy will not be considered as independent variables, and will be supposed to depend on the local shear rate and the local volume fraction only.

The main pressure load is exerted along the radial direction of the Couette device and one can refer to  $\tau_{rr}$  as the granular pressure. This granular pressure is the result of two distinct physical phenomena, multiplicity of the possible spatial configurations and impacts between grains. The many possible configurations of the grains, stemming from free-volume effects, are represented by the “disorder” pressure at the continuum level [11]. That disorder pressure depends on the solid fraction only and we write it as  $P^*F(\phi)$ . The derivative  $\partial F(\phi)/\partial\phi$  represents the rigidity of the granular medium in steady shear motion while  $(P^*/\rho_p)\partial F(\phi)/\partial\phi$  can be considered as the velocity of sound (squared). Because neither the grain elastic modulus nor any thermal energy can be involved in the disorder pressure, it is not evident to give an order of magnitude for  $P^*$ . There is some evidence that  $P^*$  is of order 1 to 100 Pa (i.e. comparable to the self-weight pressure under a few granular layers) but we consider hereafter that  $P^*$  is a constant to be determined by experiments. Besides the disorder pressure, the normal stress also includes the effects of the impacts between grains. We used the name “impact” to insist on the difference between many-body and rebound-less collisions met in dense media [12], contrasting with the more traditional two-body collisions of dilute media with  $\phi < \phi_m$ . At variance with the disorder pressure, the impact pressure is rate-dependent and on dimensional grounds must be written in the Bagnold-like form [13] so that the total granular pressure appears as

$$\tau_{rr} = P^*F(\phi) + \rho_p D^2 \mu_N(\phi) (r \partial\omega/\partial r)^2. \quad (4)$$

In this constitutive relation  $D$  is the grain size and  $\mu_N(\phi)$  represents Reynold’s dilatancy: shearing the medium at constant volume fraction creates a larger pressure and conversely, shearing the medium at constant pressure induces a decrease of the volume fraction (hence  $\mu_N(\phi)$  is expected to be positive and to increase with the volume fraction). Besides the pressure, one must give model expressions for the shear. We assume the shear stress to be the sum of a Coulomb-like solid friction and a second dissipative contribution due to the impacts between grains

$$\tau_{r\theta} = -\mu(\phi)\tau_{rr} \frac{\partial\omega/\partial r}{|\partial\omega/\partial r|} - \rho_p D^2 \mu_T(\phi) r^2 |\partial\omega/\partial r| \partial\omega/\partial r.$$

Because the local rotation rate is expected to decrease when one moves away from the inner cylinder, the above expression simplifies into

$$\tau_{r\theta} = \mu(\phi)\tau_{rr} + \rho_p D^2 \mu_T(\phi) (r \partial\omega/\partial r)^2. \quad (5)$$

In this expression  $\mu(\phi)$  is a compaction-dependent friction coefficient and  $\mu_T(\phi)$  depicts the extra dissipation due to the friction developed by sliding contacts. Because the normal stress difference  $\tau_{rr} - \tau_{\theta\theta}$  appears to have a negligible role, the modeling of the two components  $\tau_{rr}$  and  $\tau_{r\theta}$  is enough for the description of the tangential annular flow. Expressions (4) and (5) contain four positive scalar functions of the compaction. If we admit an infinite rigidity and the impossibility of any motion for  $\phi > \phi_M$ , then  $F$ ,  $\mu_N$  and  $\mu_T$  are expected to diverge for  $\phi = \phi_M$ . If we take for granted the absence of disorder pressure and dilatancy phenomena for  $\phi < \phi_m$ , then  $F$ ,  $\mu_N$  and  $\mu_T$  are expected to be very small and perhaps to vanish for  $\phi = \phi_m$  (in any case they all vanish when  $\phi < \phi_m$ ). The friction coefficient has a much smoother behavior since it is expected neither to vanish nor to become infinite in the whole range  $\phi_m \leq \phi \leq \phi_M$ . In fact  $F$ ,  $\mu_N$ ,  $\mu_T$  and  $\mu$  are functions of the *reduced solid fraction*  $\varphi$

$$\varphi = \frac{\phi - \phi_m}{\phi_M - \phi_m}, \quad (6)$$

which can be considered as some order parameter with  $\varphi = 0$  in the fluidized state and  $\varphi = 1$  in the poro-elastic state. For flows over heaps as well as over rough inclines, a satisfactory fit with experimental results could be obtained with [7]

$$F(\phi) = \text{Log} \frac{1}{1 - \varphi}, \tag{7}$$

$$\mu_N(\phi) = \frac{\mu_{N0}}{(1 - \varphi)^2}, \tag{8}$$

$$\mu_T(\phi) = \frac{\mu_{T0}}{(1 - \varphi)^2}, \tag{9}$$

$$\mu(\phi) = \mu_0. \tag{10}$$

The expression for  $F(\phi)$  is reminiscent of the configuration pressure in the lattice–gas model and it was already proposed by Savage [14]. This logarithmic expression is the only one compatible with the exponential decrease of the velocity in the deep parts of the flow over a heap [15]. The expressions of the three other functions are more debatable and the above proposals must be considered as the simplest ones.

### 3.2. Fluid-saturated granular media

When taking the role of the interstitial fluid into account, the fluid pressure  $p_f$  is supposed to be the only new source of normal stress and the fluid viscosity  $\eta_f$  is responsible for a new contribution to the shear stress. We will neglect any difference between the mean fluid velocity and the mean granular velocity in a Couette flow. The fluid strain rate is then equal to the granular strain rate  $r\partial\omega/\partial r$  and the constitutive relations (4) and (5) are modified into

$$\tau_{rr} = P^*F(\phi) + \rho_p D^2 \mu_N(\phi)(r\partial\omega/\partial r)^2 + p_f, \tag{11}$$

$$\tau_{r\theta} = \mu(\phi)(\tau_{rr} - p_f) + \rho_p D^2 \mu_T(\phi)(r\partial\omega/\partial r)^2 - \eta_f \eta(\phi) r \partial\omega/\partial r. \tag{12}$$

The transport coefficient  $\eta(\phi)$  witnesses to the influence of the solid fraction on the effective viscosity of the mixture. As shown by Bedeaux [16], the relative viscosity of a suspension of spheres can be written in the general form

$$\eta(\phi) = 1 + \frac{5\Sigma(\phi)}{2(1 - \Sigma(\phi))}$$

with  $\Sigma(\phi) = \phi + (1 - \phi_M)(\phi/\phi_M)^2$ . This expression holds in the whole range  $0 \leq \phi < \phi_M$ , but we are interested in the dense range  $\phi_m \leq \phi < \phi_M$  only. For volume fractions close to  $\phi_M$ , the above expression has the asymptotic form

$$\eta(\phi) = \frac{\eta_0}{1 - \varphi}, \tag{13}$$

where  $\eta_0 = 5\phi_M/2(2 - \phi_M)(\phi_M - \phi_m)$ , hence  $\eta_0 \approx 10\text{--}30$  for spherical grains. Since  $\phi_m$  is rather close to  $\phi_M$ , we will adopt (13) as the relative viscosity of dense granular media with  $\eta_0$  now representing the relative viscosity at the random loose packing.

## 4. Volume fraction and velocity profiles

Let us consider some horizontal plane ( $z$  fixed) somewhere between the upper and bottom surface of the granular medium. We note  $N$  and  $S$  the normal and shear stresses at the inner cylinder for that selected horizontal plane. Combining Eqs. (2) and (3) with the constitutive relations (11) and (12) results in

$$P^*F(\phi) + \rho_p D^2 \mu_N(\phi)(r\partial\omega/\partial r)^2 = P,$$

$$\mu_0 P + \rho_p D^2 \mu_T(\phi)(r\partial\omega/\partial r)^2 - \eta_f \eta(\phi) r \partial\omega/\partial r = S(r_{\text{int}}/r)^2,$$

where  $P = N - p_f$  is the *effective confining pressure*. We now take into account the above expressions for the concentration-dependent transport coefficients and deduce the two profiles of volume fraction and angular velocity

$$\phi(\rho) = \phi_M - (\phi_M - \phi_m) e^{-P/P^*} e^{g^2(\rho)}, \quad (14)$$

$$\sqrt{\frac{\mu_{N0}\rho_p D^2}{P^*}} \omega(\rho) = e^{-P/P^*} \int_{\rho}^{\rho_{\text{ext}}} g(x) e^{g^2(x)} \frac{dx}{x}. \quad (15)$$

In these two results appear  $\rho = r/r_{\text{int}}$  and  $\rho_{\text{ext}} = r_{\text{ext}}/r_{\text{int}}$  where  $r_{\text{ext}}$  is the radius of the external cylinder of the Couette setup. The external cylinder was supposed to be so rough that  $\omega(\rho_{\text{ext}}) = 0$  in all cases. The function  $g(\rho)$  is defined as

$$g(\rho) = \begin{cases} \sqrt{\frac{\mu_{N0}\sigma^*}{\mu_{T0}P^*}} \left( \sqrt{1 + \frac{S/\rho^2 - \mu_0 P}{\sigma^*}} - 1 \right) & \text{if } 1 < \rho < \sqrt{S/\mu_0 P}, \\ 0 & \text{otherwise.} \end{cases}$$

Besides the constant disorder pressure  $P^*$  appears a second characteristic stress,  $\sigma^*$ , defined from the physical properties of the grains and the interstitial fluid as

$$\sigma^* = \frac{(\eta_0 \eta_f)^2}{4\mu_{T0}\rho_p D^2}. \quad (16)$$

When  $\sigma^* \ll P^*$  the role of the interstitial fluid is negligible and the medium can be referred to as a “dry” granular medium. On the contrary, when  $\sigma^* \gg P^*$  one has a viscous-like granular medium. It is worthy to note that

$$\sqrt{\frac{\mu_{T0}P^*}{\mu_{N0}\sigma^*}} = St = \frac{T_V}{T_D}, \quad (17)$$

where  $St$  is the Stokes number (see [17] for its counterpart in avalanches), this number being in our model the ratio of the viscous regime characteristic time  $T_V = 2\mu_{T0}\rho_p D^2/(\eta_0 \eta_f)$  and the dry regime characteristic time  $T_D = \sqrt{(\mu_{N0}\rho_p D^2)/P^*}$ . Note also that our non-dimensional angular velocity in (15) bears some resemblance with  $I = \sqrt{(\rho_p D^2/P)}\omega$  proposed by the GDR MiDi [18]. The main difference is our use of the (constant) disorder pressure  $P^*$  instead of the full normal stress  $P$ . Let us define

$$r_{\text{out}} = r_{\text{int}} \sqrt{\frac{S}{\mu_0 P}}. \quad (18)$$

Since  $g(\rho)$  vanishes when  $r > r_{\text{out}}$ , this means that the shear band has a width  $r_{\text{out}} - r_{\text{int}}$  and that outside this shear band the medium is motionless with a constant volume fraction depending on  $P/P^*$ . It is quite possible that  $r_{\text{out}} > r_{\text{ext}}$ . In this case the grains move all over the gap. Everything happens as if the shear localization had disappeared while, in fact, it could still be observed using a Couette cell with a larger gap between the two cylinders. Note that the width of the shear band is proportional to  $r_{\text{int}}$  and is independent of the grain size. This should not be a surprise because when  $r_{\text{int}}$  increases to infinity the Couette cell is transformed into a plane shear cell (with vertical planes) for which the symmetry precludes any shear localization.

To induce a motion in the dense granular medium requires that  $S > \mu_0 P$  at the inner cylinder. The larger the difference  $S - \mu_0 P$ , the larger will be  $\omega(r_{\text{int}})$  but the smaller will be the volume fraction at the inner cylinder. Our model however is specially devoted to dense granular materials with  $\phi > \phi_m$  everywhere. For the medium to be dense all over the Couette cell the shear stress at the inner cylinder must not exceed some maximum value and we will limit our analysis of the Couette flow to applied shear stresses in the range

$$\mu_0 P < S < \left( \mu_0 + \frac{\mu_{T0}}{\mu_{N0}} \right) P + 2\sqrt{\sigma^*} \sqrt{\frac{\mu_{T0}}{\mu_{N0}}} P, \quad (19)$$

which amounts to  $0 < g^2(1) < P/P^*$ . As a consequence, the width of the shear band has some maximum value and for a dry granular material

$$r_{\text{out}} < r_{\text{int}} \sqrt{1 + \frac{\mu_{T0}}{\mu_0 \mu_{N0}}}. \quad (20)$$

The maximum value is independent of the particle size and since the ratio  $\mu_{T0}/\mu_{N0}$  is very close to  $\mu_0$  [7], the maximum width is about half the radius of the inner cylinder. For liquid-saturated granular media the maximum width also depends on  $\sigma^*/P$  and is always larger than for dry granular media.

### 5. Model predictions

We now consider two mutually exclusive situations that are typical of most experiments with a Couette cell. In the first one, the confining pressure of any horizontal layer is kept constant. In the second one, the mean volume fraction of any horizontal layer is kept constant.

#### 5.1. Experiments with a constant confining pressure

Operating at a constant confining pressure  $P_0$  while changing the driving shear requires that no part of the apparatus prevents the grains from moving in the vertical direction and that the fluid is allowed to drain out of the granular material. Motion begins when the shear stress at the inner cylinder is just above the minimum value  $S_{\min} = \mu_0 P_0$ . When  $P$  is replaced by  $P_0$  in (14) and (15) one solves them to get the volume fraction profile and the velocity profile. Figs. 1 and 2 represent these profiles for different values of the shear stress at inner cylinder. Note that the radius  $r_{\text{ext}}$  of the external cylinder has no influence on the volume fraction profile. It has also no influence on the velocity profile

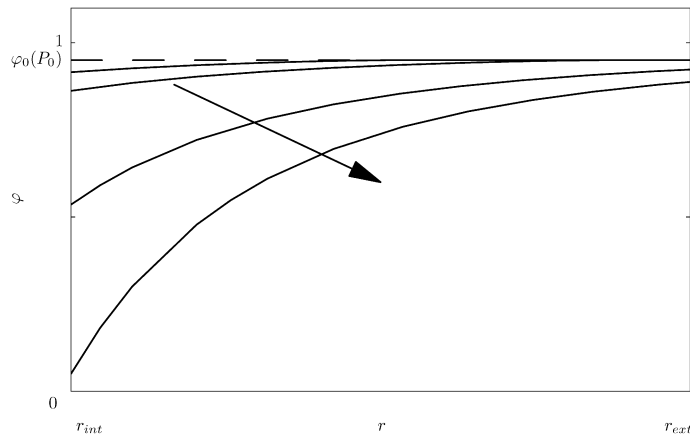


Fig. 1. Reduced solid fraction profiles of wet granular materials for increasing shears (in the direction of the arrow) and a fixed pressure  $P_0$ .

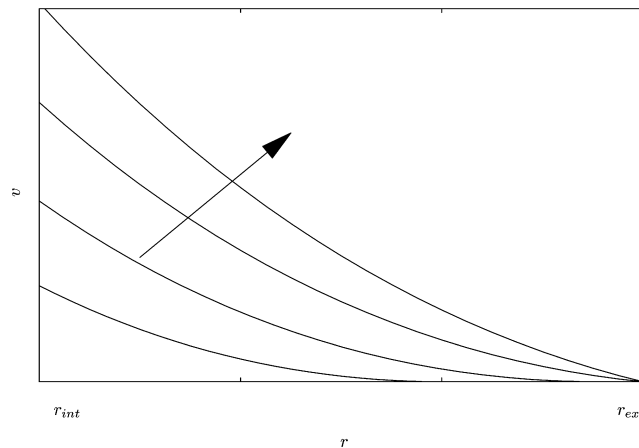


Fig. 2. Velocity profiles for increasing shear stresses (in the direction of the arrow) at internal cylinder and a fixed pressure. For the two largest shear stresses the motion extends over the whole gap.

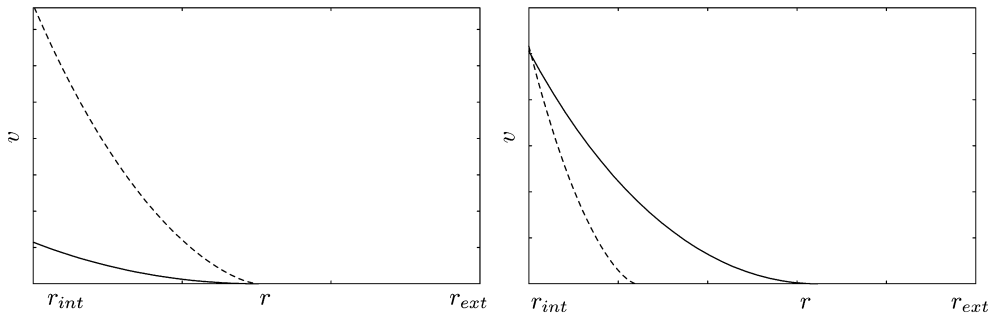


Fig. 3. Velocity profile of a dry material (dashed line), and of a liquid-saturated material (plain line). Left, for a given applied shear stress, the velocity at the inner cylinder is smaller for the wet material. Right, for a given velocity at the inner cylinder, the shear band of the wet material is larger.

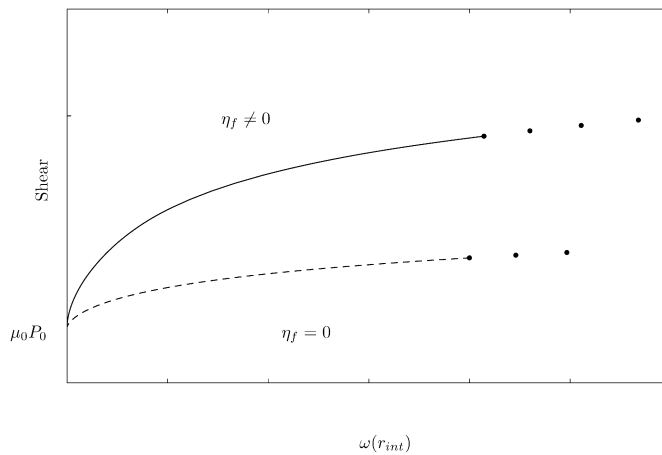


Fig. 4. Driving shear versus angular velocity at inner cylinder for liquid-saturated (plain line) and dry (dashed line) materials and a constant confining pressure  $P_0$ .

for low shears, when the width of the shear band is smaller than the gap between the two cylinders. But as soon as the shear exceeds the value

$$S_{\text{gap}} = \mu_0 P_0 \left( \frac{r_{\text{ext}}}{r_{\text{int}}} \right)^2 \tag{21}$$

then the flow invades the whole gap between the two cylinders and the boundary condition  $\omega(r_{\text{out}}) = 0$  is replaced by  $\omega(r_{\text{ext}}) = 0$ , as is expected when the external cylinder is rough enough to prevent any slip on it. Fig. 3(left) compares the velocity profile of the dry medium with that of a liquid-saturated medium for equal shear stresses at the inner cylinder while Fig. 3(right) compares the two media for equal velocities at the inner cylinder. In Fig. 4 is plotted the velocity at the inner cylinder as a function of the driving shear, for a liquid-saturated and for a dry material. The dotted parts of the curves correspond to driving shears so large that the compaction at the inner cylinder is smaller than  $\phi_m$ , outside the concentrations described by our model. Hence, working with dense granular media limits the driving shears to the range given by (19) with  $P = P_0$ . The maximum shear stress increases with  $\sigma^*$  as can also be seen in Fig. 4. In most Couette cells shear localization has always been observed for dry materials which means that most devices are such that  $S_{\text{gap}}$  is larger than the maximum possible  $S$  (when  $\sigma^* = 0$ ) implying that  $(r_{\text{ext}}/r_{\text{int}})^2 > 1 + \mu_{T0}/\mu_0\mu_{N0}$ . However, because the maximum possible shear increases with  $\sigma^*$  it is quite possible that for the same granular material filled with a liquid of large viscosity the rotation of the inner cylinder is able to induce a motion all over the gap (as was in fact supposed for the two largest shears of Fig. 2).

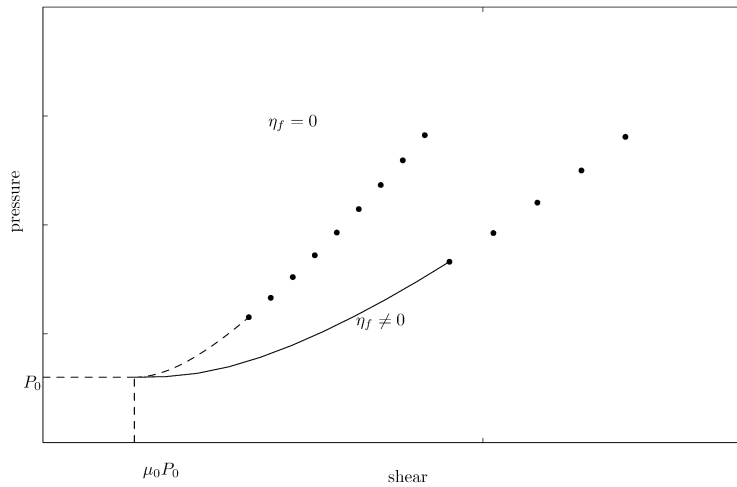


Fig. 5. When the total volume (or mean volume fraction) is kept constant, the pressure increase is larger for dry materials (dashed line) than for liquid-saturated ones (plain line);  $P_0$  is the initial confining pressure.

### 5.2. Experiments with constant mean volume fraction

In these experiments a top plate prevents the grains to move in the vertical direction and the gap between the two cylinders is kept fixed. Conservation of the mass (volume) of the grains in a horizontal layer expresses as

$$2\pi \int_{r_{\text{int}}}^{r_{\text{ext}}} r \phi(r) dr = \pi (r_{\text{ext}}^2 - r_{\text{int}}^2) \phi_0, \tag{22}$$

where  $\phi_0$  is the initial (and assumed uniform) volume fraction of the granular medium, associated with the initial confining pressure  $P_0$ . When the applied shear is larger than the minimum value  $S_{\text{min}} = \mu_0 P_0$ , the medium is put into motion, its volume fraction close to the inner cylinder decreases. Since the total volume of grains in a horizontal layer is assumed to be conserved, the solid fraction must increase above  $\phi_0$  in the outer part of the cell and this requires an increase of the confining pressure above its initial value  $P_0$ . In fact, the confining pressure increases with the driving shear and the relationship  $P(S)$  is deduced from the above mass (or volume) conservation equation as the solution of

$$2 \int_1^{\rho_{\text{ext}}} \rho e^{g^2(\rho)} d\rho = (\rho_{\text{ext}}^2 - 1) e^{(P-P_0)/P^*}. \tag{23}$$

Since the integral is finite, when  $\rho_{\text{ext}} = r_{\text{ext}}/r_{\text{int}}$  is very large the pressure is almost constant and equal to  $P_0$ . To obtain results markedly different from those found in the constant pressure case, we must consider small ratios  $r_{\text{ext}}/r_{\text{int}}$ , of order 1.5 to 2 which are values typical of most Couette devices. The confining pressure is presented in Fig. 5 for dry and liquid-saturated materials. The maximum possible shear is larger than its value at constant pressure. In Fig. 6 is represented the velocity at the inner cylinder as a function of the driving shear. It is worthy to note that above some minimal shear, a (quasi-)linear relationship exists between the velocity at the inner cylinder and the driving shear, in contrast with what happens in the constant pressure case represented in Fig. 4.

### 5.3. Comparison with experimental results

The predictions of the model are now compared to the experimental results presented in Huang et al. [5] and Ovarlez et al. [6]. The size of the Couette cell is such that  $r_{\text{ext}}/r_{\text{int}} = 1.45$ . The grains are spherical polystyrene beads with diameter  $D = 0.29 \times 10^{-3}$  m and a mass density  $\rho_p = 1.04 \times 10^3$  kg m<sup>-3</sup>. The shear stress for incipient motion is between 1 Pa and 3 Pa. Since the macroscopic friction coefficient is  $\mu_0 \approx 0.40$ , the initial confining pressure is between 2.5 Pa and 7.5 Pa. Hence,  $P_0$  has the same order of magnitude as  $P^*$  which is expected to be in the range

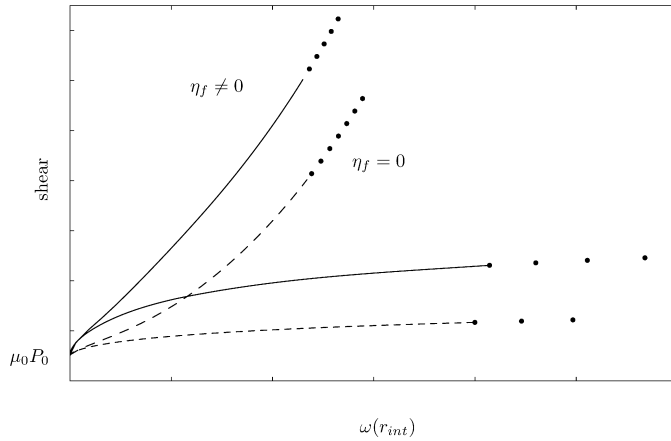


Fig. 6. Driving shear versus angular velocity at inner cylinder for liquid-saturated (plain line) and dry (dashed line) materials at constant confining volume.  $P_0$  is the initial confining pressure. For comparison with the constant pressure case, the two lower curves reproduce those of Fig. 4.

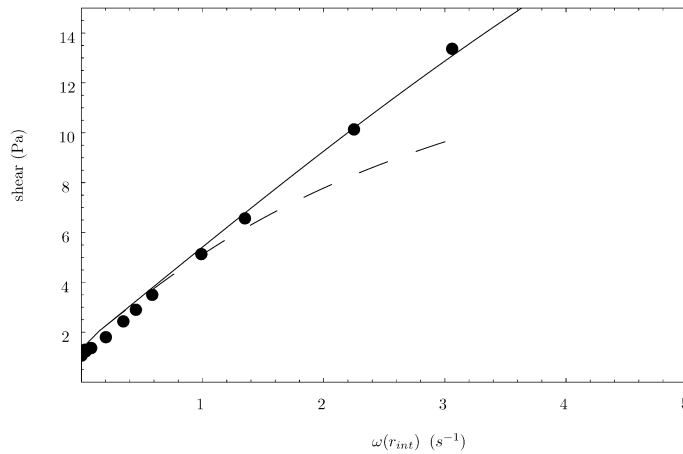


Fig. 7. Relation between the angular velocity and the shear at the inner cylinder. Dots are experimental results from [5], plain line is the prediction for constant volume and dashed line is the prediction for constant pressure.

1–100 Pa. Most of the experiments used a fluid with a viscosity  $\eta_f = 20 \times 10^{-3}$  Pa s for which  $\sigma^* \approx 100$  Pa if  $\eta_0 \approx 10$  and  $\mu_{T0} \approx 1$ . We deduce that the experiments were performed under the condition  $\sigma^* \gg P^*$ , i.e. with a viscous-like granular medium. Figs. 7 and 8 compare the experimental results for the “flow curve” (i.e. shear stress  $S$  as a function of the angular velocity  $\omega(r_{int})$  of the rotating cylinder) with the model predictions for the two operating conditions, constant pressure on the one hand and constant volume on the other hand. The experimental results appear to be better fitted by the constant volume curve. The best fit was obtained with  $\mu_{N0} = 2$ ,  $\mu_{T0} = 1$ ,  $P^* = 3$  Pa,  $\sigma^* = 120$  Pa and  $P_0 = 7.8$  Pa. However, with the above best-fit values for the model parameters we have found a width of the shear band which seems too large when  $\omega(r_{int}) > 1$  rad/sec. For these relatively high rotating velocities the centrifugal forces possibly play a role and the granular pressure, as suggested by (1), is likely to increase when moving away from the rotating cylinder. As a consequence, the excess shear stress  $S/\rho^2 - \mu_0 P(\rho)$  will vanish at a position  $r_{out}$  closer to the rotating cylinder than the position predicted in (18) for a spatially uniform  $P$ . There is in fact a second discrepancy with the experimental results which concerns the solid fraction profile. We predicted that  $\phi(r)$  depends on  $\omega(r_{int})$  while the experiments conclude to a quasi-independence of the two quantities. This is an intriguing experimental result because it means that the same profile will also be observed for the quasi static granular medium and it suggests some long-lasting influence of the state in which the medium was initially prepared. It is quite possible that the solid fraction needs a very long equilibration time (a few hours and perhaps a few days) before it takes its true steady profile. A third discrepancy concerns the dry media. We predicted that the band width  $r_{out} - r_{int}$  increases with  $\omega(r_{int})$

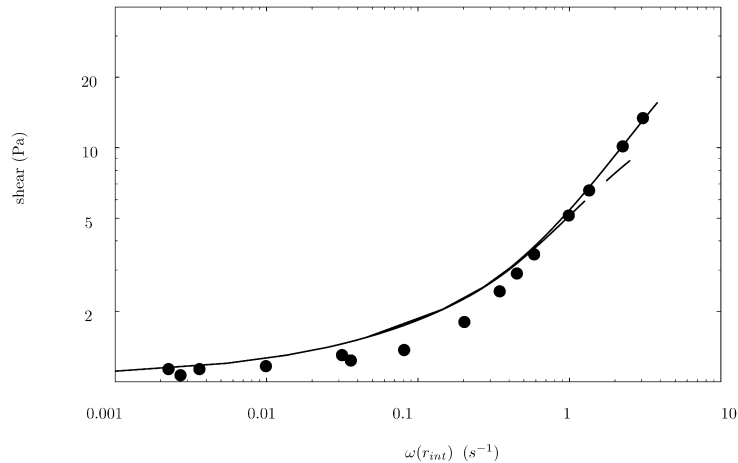


Fig. 8. Same results as in Fig. 7 but with two logarithmic scales to insist on the slight discrepancy that exists at intermediate angular velocities.

while most of the experiments [1,3] concluded that the width is of the order of a few diameters and independent of the velocity of the rotating cylinder. Here again, we can refer to the difficulty of obtaining a true steady state for the solid fraction profile, but this is not the only explanation: we neglected the extra friction provided by the top and the bottom plates which results in a shear stress decreasing faster than  $S/\rho^2$ , and is likely to flatten the dependence on  $\omega(r_{int})$  of the band width. The results the above analysis are thus restricted to very high Couette setups operating at relatively small angular velocities.

## 6. Conclusions

We have proposed a rheological model for the steady flow of dense and fluid-saturated granular media, in which the two main parameters are two characteristic stresses. The first one,  $P^*$ , witnesses to the disorder (or free-volume) entropy that exists in media with solid fractions between the random loose and the random close packings. Previous estimates [11] suggested that  $P^*$  is of order 1–100 Pa which happens to be the order of magnitude of  $\rho_p g D$ . Note however that  $P^*$  is a constant while  $\rho_p g D$  is not. Hence we were not justified in writing  $P^* \propto \rho_p g D$  like we did in previous publications [7]. The second characteristic stress,  $\sigma^*$  defined in (16), is built from the physical parameters of both the grains and the interstitial fluid. Dry granular media correspond to  $\sigma^* \ll P^*$  while  $\sigma^* \gg P^*$  holds for viscous-like granular media. For the disorder pressure to be a pertinent quantity, the granular medium must be able to explore all the microstates involved in the disorder entropy. As a consequence the disorder pressure is certainly relevant to steady flows and we considered here the steady Couette flow between two rotating cylinders. In this particular geometry, flow localization is the consequence of the sign-reversal of the excess shear  $S/\rho^2 - \mu_0 P(\rho)$  at some position  $r_{out}$  in the gap between the two cylinders. When  $P$  is uniform over any horizontal plane,  $r_{out}$  is given in (18). The two main model predictions concern the solid fraction and the velocity profiles as given in (14) and (15). The predictions for the velocity profiles are in rather good agreement with experimental profiles obtained with either dry or wet granular media. The solid fraction profile is predicted to decrease close to the rotating cylinder and the magnitude of the depletion (as well as the width of the shear band) is predicted to increase with the velocity of the rotating cylinder, while experiments concluded to a quasi-independence. We suggested these discrepancies could be traced to the very long time needed for the solid fraction to come to its final steady state. When these very long transients are not properly taken into account, the solid fraction remembers the way the medium was prepared and can be markedly different from its true steady value. It is also possible that the present rheological model is wrong because nothing like the disorder pressure exists in the real life of granular materials. This would imply to very disappointing conclusions (a) Bagnold's rheology holds for all solid fractions, from zero up to the random close packing and (b) the recent statistical approach of granular matter [19] has absolutely no incidence on the rheology. We preferred here to bet on the existence of  $P^*$ !

## References

- [1] C.T. Veje, D.W. Howell, R.P. Berhinger, Kinematics of a two-dimensional granular Couette experiment at the transition to shearing, *Phys. Rev. E* 59 (1999) 739–745.
- [2] L. Bocquet, W. Losert, D. Schalk, T.C. Lubenski, J.P. Gollub, Granular shear flow dynamics and forces: Experiments and continuum theory, *Phys. Rev. E* 65 (2002) 011307.
- [3] D.M. Mueth, G.F. Debregeas, G.S. Karczmar, P.J. Eng, S.R. Nagel, H.M. Jaeger, Signatures of granular microstructure in dense shear flows, *Nature* 406 (2000) 385–389.
- [4] F. Da Cruz, *Écoulements de grains secs: frottement et blocage*, PhD thesis, École Nationale des Ponts et Chaussées, 2004. Available from <http://pastel.paristech.org/archive/00000946/>.
- [5] N. Huang, G. Ovarlez, F. Bertrand, S. Rodts, P. Coussot, D. Bonn, Flow of wet granular materials, *Phys. Rev. Lett.* 94 (2005) 028301.
- [6] G. Ovarlez, F. Bertrand, S. Rodts, Local determination of the constitutive law of a dense suspension of non-colloidal particles through MRI, Preprint, 2005.
- [7] C. Josserand, P.-Y. Lagrée, D. Lhuillier, Stationary shear flows of dense granular materials: a tentative continuum modelling, *Eur. Phys. J. E* 14 (2004) 127–135.
- [8] S.B. Savage, Granular flows down rough inclines: review and extension, in: J.T. Jenkins, M. Satake (Eds.), *Proceedings of the US–Japan Seminar on New Models and Constitutive Relations in the Mechanics of Granular Materials*, Elsevier Science Publishers, Amsterdam, 1982, pp. 261–282.
- [9] P.C. Johnson, R. Jackson, Frictional-collisional constitutive relations for granular materials, with application to plane shearing, *J. Fluid Mech.* 176 (1987) 67–93.
- [10] C. Ancey, P. Evesque, Frictional-collisional regime for granular suspension flows down an inclined channel, *Phys. Rev. E* 62 (2000) 8349–8360.
- [11] C. Josserand, P.-Y. Lagrée, D. Lhuillier, Granular pressure and the thickness of a layer jamming on a rough incline, *Europhys. Lett.* 73 (3) (2006) 363369.
- [12] J. Rajchenbach, Dense, rapid flows of inelastic grains under gravity, *Phys. Rev. Lett.* 90 (2003) 144302.
- [13] R.A. Bagnold, *The Physics of Sediment Transport by Wind and Water: A Collection of Hallmarks Papers by R.A. Bagnold*, The American Society of Civil Engineers, New York, 1988. Edited by C.R. Thorne, R.C. MacArthur, J.B. Bradley.
- [14] S.B. Savage, Analysis of slow high-concentration flows of granular materials, *J. Fluid Mech.* 377 (1998) 1–26.
- [15] T.S. Komatsu, S. Inagaki, N. Nakagawa, S. Nasuno, Creep motion in a granular pile exhibiting steady surface flow, *Phys. Rev. Lett.* 86 (2001) 1757–1760.
- [16] D. Bedeaux, The effective viscosity for a suspension of spheres, *J. Colloid Interface Sci.* 118 (1987) 80–86.
- [17] S. Courrech du Pont, P. Gondret, B. Perrin, M. Rabaud, Granular avalanches in fluids, *Phys. Rev. Lett.* 90 (2003) 044301.
- [18] GDR MiDi, On dense granular flows, *Eur. Phys. J. E* 14 (2004) 341.
- [19] S.F. Edwards, R.B. Oakeshott, Theory of powders, *Physica A* 157 (1989) 1080–1090.